Journal Pre-proof

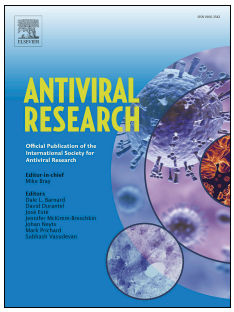

The broad spectrum antiviral ivermectin targets the host nuclear transport importin α/β1 heterodimer

Sundy N.Y. Yang, Sarah C. Atkinson, Chunxiao Wang, Alexander Lee, Marie A. Bogoyevitch, Natalie A. Borg, David A. Jans

PII: S0166-3542(19)30721-1

DOI: https://doi.org/10.1016/j.antiviral.2020.104760

Reference: AVR 104760

To appear in: *Antiviral Research*

Received Date: 18 December 2019

Revised Date: 28 February 2020

Accepted Date: 28 February 2020

Please cite this article as: Yang, S.N.Y., Atkinson, S.C., Wang, C., Lee, A., Bogoyevitch, M.A., Borg, N.A., Jans, D.A., The broad spectrum antiviral ivermectin targets the host nuclear transport importin α/β1 heterodimer, *Antiviral Research* (2020), doi: https://doi.org/10.1016/j.antiviral.2020.104760.

THE BROAD SPECTRUM ANTIVIRAL IVERMECTIN TARGETS THE HOST NUCLEAR TRANSPORT IMPORTIN α/β1 HETERODIMER

Sundy N.Y. Yang[a], Sarah C. Atkinson[b], Chunxiao Wang[a], Alexander Lee[a], Marie A. Bogoyevitch[c], Natalie A. Borg[bd] and David A. Jans[a#]

[a]Nuclear Signalling Laboratory, Monash Biomedicine Discovery Institute and Department of Biochemistry and Molecular Biology, Monash University, Clayton, Vic. 3800, Australia; [b]Infection and Immunity Program, Monash Biomedicine Discovery Institute and Department of Biochemistry and Molecular Biology, Monash University, Clayton, Vic. 3800, Australia; [c]Department of Biochemistry and Molecular Biology, University of Melbourne, Melbourne, Australia; [d]Current address, Immunity and Immune Evasion Laboratory, Chronic Infectious and Inflammatory Diseases Research, School of Health and Biomedical Sciences, RMIT University, Bundoora, Vic. 3083, Australia

[#]Corresponding author, c/- Nuclear Signalling Laboratory, Monash Biomedicine Discovery Institute and Department of Biochemistry and Molecular Biology, Monash University, Clayton, Vic. 3800, Australia; Tel. 613 9902 9341; email David.Jans@monash.edu

Running Title: Ivermectin targets the IMPα/β1 heterodimer

Keywords: flavivirus, nuclear transport inhibitors, importins, viral infection, West Nile Virus, dengue virus, Zika virus,

ORCID ID#: D.A. Jans ORCID ID#0000-0001-5115-4745

ABSTRACT

Infection by RNA viruses such as human immunodeficiency virus (HIV)-1, influenza, and dengue virus (DENV) represent a major burden for human health worldwide. Although RNA viruses replicate in the infected host cell cytoplasm, the nucleus is central to key stages of the infectious cycle of HIV-1 and Influenza, and an important target of DENV nonstructural protein 5 (NS5) in limiting the host antiviral response. We previously identified the small molecule ivermectin as an inhibitor of HIV-1 integrase nuclear entry, subsequently showing ivermectin could inhibit DENV NS5 nuclear import, as well as limit infection by viruses such as HIV-1 and DENV. We show here that ivermectin's broad spectrum antiviral activity relates to its ability to target the host importin (IMP) α/β1 nuclear transport proteins responsible for nuclear entry of cargoes such as integrase and NS5. We establish for the first time that ivermectin can dissociate the preformed IMPα/β1 heterodimer, as well as prevent its formation, through binding to the IMPα armadillo (ARM) repeat domain to impact IMPα thermal stability and α-helicity. We show that ivermectin inhibits NS5-IMPα interaction in a cell context using quantitative bimolecular fluorescence complementation. Finally, we show for the first time that ivermectin can limit infection by the DENV-related West Nile virus at low (μM) concentrations. Since it is FDA approved for parasitic indications, ivermectin merits closer consideration as a broad spectrum antiviral of interest.

1. Introduction

Infection by RNA viruses such as human immunodeficiency virus (HIV)-1, influenza, and dengue virus (DENV) represents a major burden for human health worldwide. In 2017, for example, there were almost 37 million people living with HIV-1, with close to 1 million deaths for AIDS related disease (Ortblad et al., 2013; GBD 2015 HIV Collaborators, 2016; WHO, 2018). Respiratory diseases from seasonal influenza is associated with up to 650,000 deaths annually (Nair et al., 2011; WHO, 2018), while c. 70% of the world's population in over 120 countries is currently threatened by flaviviral infection, with an estimated 100 million symptomatic DENV infections and up to 25,000 deaths each year (Brady et al., 2012; Bhatt et al., 2013). Viruses remain the least well understood of human pathogens, the patent lack of knowledge with respect to pathogenic mechanisms and host-parasite interactions being highlighted by the general lack of effective drugs against viruses and limited success in developing vaccines. Problems with respect to antiviral therapeutics include high cost of production, limitations in availability, and a high prevalence of resistance e.g. among patients receiving antiretroviral drugs (GBD 2015 HIV Collaborators, 2016).

Antivirals that can limit infection by a broad spectrum of different viruses generally need to be host-directed, i.e. they need to target a host factor/function required for infection by disparate viruses. Although RNA viruses do not replicate in the infected host cell nucleus, the nucleus is central to key stages of the infectious cycle of HIV-1 and influenza (Caly et al., 2012), and a key target of other RNA viruses such as DENV and West Nile Virus (WNV), where nuclear targeting of nonstructural protein 5 (NS5) is central to limiting the host antiviral response; specific inhibitors or mutations preventing NS5 nuclear import significantly limit virus production (Pryor et al., 2007; Wagstaff et al., 2012; Tay et al., 2013; Fraser et al., 2014; Lopez-Denman et al., 2018; see Martin and Jans, 2018). NS5's role in the host nucleus appears to be to suppress the host antiviral response (Medin et al., 2005; Pryor et al., 2007; Rawlinson et al., 2009) in part through effects on mRNA splicing (de Maio et al., 2016), and potentially through effects on subnuclear bodies/immune signalling (Ng et al. 2019; Giovannoni et al., 2019; see Tan et al., 2019). The clear implication is that viral protein nuclear access has important potential as a target for therapeutic intervention.

We originally identified the small molecule ivermectin as an inhibitor of recognition of HIV-1 integrase (IN) by the importin (IMP) α/β1 heterodimer responsible for IN nuclear import (Wagstaff et al., 2011), subsequently establishing ivermectin's ability to inhibit integrase nuclear import and HIV-1 replication (Wagstaff et al., 2012). Although other actions of ivermectin have reported, including those targeting DENV NS3 helicase (Mastrangelo et al., 2012), ivermectin has been clearly shown to inhibit nuclear import of host (eg. Kosyna et al., 2015; van der Watt et al., 2016) and viral proteins, including simian virus SV40 large tumour antigen (T-ag) and DENV NS5. Importantly, it has been demonstrated to limit infection by a number of viruses, including HIV-1, DENV serotypes 1-4, and influenza (Wagstaff et al., 2012; Tay et al., 2013; Lundberg et al., 2013; Goetz et al., 2016; Atkinson et al., 2018; Shechter et al., 2018), with this broad spectrum activity believed to be due to the reliance by many different RNA viruses on IMPα/β1 during infection (Caly et al, 2012; Jans et al., 2019).

Here we characterise the mechanism of action of ivermectin for the first time, establishing that it is able to bind to the IMPα armadillo (ARM) repeat domain, leading to effects on IMPα thermal stability and α-helicity that prevent binding to IMPβ1. Importantly, ivermectin is also able to dissociate preformed IMPα/β1 heterodimer, and we use quantitative bimolecular fluorescence complementation to show that this inhibits NS5-IMPα interaction in a cell context. Finally, we show

that ivermectin has strong antiviral activity against the DENV-related WNV (EC_{50} of < 1 μM), as well as Zika virus (ZIKV) (Asian/Cook Islands/2014 strain). With its established safety profile for human use (Jans et al., 2019; Gonzales Canga et al., 2008; Munoz et al., 2018), ivermectin represents an exciting possibility as a broad spectrum antiviral, particularly for flaviviruses.

2. Results

2.1 Ivermectin inhibits binding of IMPα to IMPβ1 and dissociates the IMPα/β1 heterodimer

We previously identified ivermectin as an inhibitor of HIV-1 IN-IMPα/β1 interaction, subsequently showing inhibition of IMPα/β binding to SV40 T-ag (Wagstaff et al., 2011), as well as DENV2 NS5 (Wagstaff et al., 2011, 2012), with a half maximal inhibitory concentration (IC_{50}) of c. 2 μM (Supp. Fig. 1, Table 1); we also showed it could block NS5 nuclear localisation in DENV-infected cells (Tay et al., 2013). Since ivermectin appears to inhibit IMPα/β1 interactions generally, rather than being specific to a particular viral protein, we hypothesised that ivermectin may target the IMPα/β1 heterodimer. To investigate this formally, we initially tested for the first time whether ivermectin could inhibit binding of recombinant IMPα to IMPβ1 using an established ALPHAscreen binding assay. Strikingly, ivermectin was not only able to inhibit IMPα-IMPβ1 interaction (IC_{50} of 6 μM), but was also capable of dissociating preformed IMPα/β1 heterodimer (IC_{50} value of c. 6.5 μM; Fig. 1A, Table 1). The clear implication was that ivermectin's impact on IMPα/β1 recognition of viral and other proteins is through dissociating the heterodimer itself/preventing its formation. The control molecule budenoside, previously reported to be a specific inhibitor of HIV-1 IN recognition by IMPα/β1, as well as IN nuclear import (Wagstaff et al., 2018), was tested in parallel, but did not inhibit the IMPα-IMPβ1 interaction or dissociate the IMPα/β1 heterodimer (Fig. 1A), consistent with the idea that budenoside targets IN directly, rather than the IMPα/β1 heterodimer (Wagstaff et al., 2011. 2018).

These results were confirmed using sedimentation velocity analytical ultracentrifugation (AUC) (Yang et al., 2019) (Fig. 1B; see also Supp. Fig. 2). In the absence of ivermectin, IMPα, IMPβ1 as well as the IMPα/β1 heterodimer all sediment as single species with sedimentation coefficients ($s_{20,w}$) of 3.5, 5.3 and 6.7S respectively (Fig. 1B; see Supp. Table 1) [26]. When the IMPα/β1 heterodimer was incubated with 12.5 μM ivermectin, a clear increase in the ratio of free IMPα to IMPα/β1 was observed (Fig. 1B), consistent with dissociation of the heterodimer; this ratio was further increased at 50 μM ivermectin (Fig. 1B). Budenoside had no such effect on the IMPα/β1

heterodimer (Fig. 1B, bottom). Taken together, the results were consistent with the idea that ivermectin can dissociate the IMPα/β heterodimer.

2.2 Ivermectin binds to the IMPα ARM repeat domain with effects on thermostability

To confirm direct binding of ivermectin to IMP and determine whether the compound interacts with IMPα or IMPβ1, we tested the effect of ivermectin binding on IMPα, IMPαΔIBB (a truncated form of IMPα consisting of ARM repeats, but lacking the autoinhibitory IMPβ1-binding domain) and IMPβ1 in thermostability assays (Yang et al., 2019). All proteins showed thermostability maxima between 40 and 45^{o}C, as previously (Yang et al., 2019); strikingly, the thermostability of IMPα and IMPαΔIBB but not IMPβ1 was markedly decreased in the presence of concentrations of ivermectin > 70 μM, with unfolding evident at temperatures as low as c. 35^{o}C (Fig. 2A left panel). Underlining the specificity of the results was the lack of effect of ivermectin on the RNA dependent RNA polymerase domain (RdRp) from ZIKV or DENV, consistent with lack of binding to either of these proteins (Fig. 2A, bottom left panel). Similarly, the NS5 targeting agent 4-HPR (*N*-(4-hydroxyphenyl) retinamide) had no effect on the thermostability of IMPαΔIBB (Fig. 2A, top right panel), consistent with lack of binding to IMPα; this was in stark contrast to its destabilising effect on DENV RdRp (Fig. 2A, top right panel; see also Yang et al., 2019). The clear implication is that ivermectin binds IMPα directly, most likely within the ARM repeat domain, to impact IMPα structure.

Far-UV circular dichroism (CD) spectroscopy was performed to confirm the structural changes induced by ivermectin binding to IMPα and IMPαΔIBB. The CD spectra for IMPα and IMPαΔIBB displayed double minima at 208 and 222 nm (Supp. Fig. 3), consistent with IMPα's predominantly α-helical structure (Kobe, 1999; Yang et al., 2019); IMPβ1 showed comparable spectra (minima at 210 and 220 nm). Ivermectin reduced the α-helical content of both IMPα and IMPαΔIBB by c. 15 %, but had no effect on IMPβ1 (Fig. 2B; Supp. Fig. 3A-C; Supp. Table 2). In stark contrast, both the control molecules 4-HPR and budenoside had no such effect (Supp. Fig. 3D-I; Supp. Table 2). The results overall are consistent with the idea that ivermectin can bind directly to the ARM repeat domain of IMPα to alter structure/conformation; presumably this represents the basis for inhibited binding to IMPβ1.

2.3 Ivermectin can prevent IMPα-NS5 binding in a cellular context

The above results indicate that ivermectin acts by binding to IMPα to impact its conformation and thereby prevent its ability to bind nuclear import cargoes. As a first step to confirm this in a cellular context for DENV NS5, we exploited the bimolecular fluorescence complementation (BiFc) experimental approach that is based on reconstituting Venus protein fluorescence through specific protein-protein interaction bringing the Venus N-terminal (VN-) and C-terminal (VC-) fragments into close proximity (Kodama et al., 2010). The BiFc system enables detection of interactions with minimal perturbance to the cells, requires no assumptions about the accessibility of the complex to extrinsic fluorophores, and is sufficiently sensitive to enable analysis of interactions between proteins expressed at levels comparable to endogenous proteins (Kerppola et al., 2008). Importantly, BiFC analysis allows the detection of interactions that may involve only a subpopulation of a particular protein (such as IMPα), which can specifically interact with many cellular proteins (Hu et al., 2002). Specific interaction between binding partners in the system result in a robust fluorescent signal through reconstituted Venus, whereas lack of interaction results in a low signal; results illustrating this for the control Fos-Jun interacting pair (Patel et al., 1994) are shown in Supp. Fig. 4, where robust signal is evident for full length Fos, but not for Fos lacking the bZIP domain responsible for binding (Supp. Fig. 4A). Quantitative analysis for the specific nuclear fluorescence (nuclei identified by Hoechst staining - see Methods section) confirms significantly ($p < 0.0001$) 5-fold reduced interaction in the absence of the bZIP domain (Supp. Fig. 4A).

We next generated expression constructs in the BiFc system for NS5, together with those for IMPα and IMPαΔIBB (see Methods section). We also generated an additional NLS-containing control construct encoding 4 tandem copies of SV40 T-ag amino acids 111-135, including the well-characterised NLS (amino acids 126-132) (Huebner et al., 1997; Xiao et al., 1997). NS5, like the 4XNLS control, showed robust interaction with IMPα in the system (Fig. 3A, top row of panels), as well as with IMPαΔIBB (Fig. 3A, third row of panels), consistent with NLS recognition in the cellular context. To test the ability of ivermectin to perturb NLS recognition by IMPα in a cellular context, we treated cells in parallel with ivermectin overnight, and then imaged the next day. Ivermectin treatment resulted in greatly reduced nuclear fluorescence in the case of NS5 and the 4XNLS construct with both IMPα and IMPαΔIBB (Fig. 3A, 2nd and 4th rows of panels). All results were confirmed by quantitative analysis, revealing significantly ($p < 0.01$) 60-80% reduced interaction upon overnight incubation with ivermectin in the case of NS5 (Fig. 3B, right); analysis for 4XNLS was comparable, with significantly ($p < 0.05$) 30-40% reduced interaction induced by ivermectin (Fig. 3B left). Parallel experiments (Supp. Fig. 4B) for the Fos-Jun control pair showed a lack of inhibition of interaction, consistent with the specificity of the effect of ivermectin for IMPα-

interactions. Results overall indicate that ivermectin is able to inhibit recognition by IMPα of NLS-containing proteins such as NS5 in a cell context.

2.4 Ivermectin can inhibit WNV, as well as DENV and ZIKV

We previously showed that ivermectin limits infection by all four serotypes of DENV (Wagstaff et al., 2012; Tay et al., 2013), while other studies imply that infection by several strains of ZIKV may also be limited by ivermectin (eg. see Barrows et al., 2016). We decided to test efficacy towards WNV by examining ivermectin's ability to inhibit infection by WNV (Kunjin; MRM61C strain); in parallel we tested ivermectin's ability to limit infection by ZIKV (Asian/Cook Islands/2014, a strain not previously tested for ivermectin sensitivity), as well as DENV-2 (New Guinea C; M29095, Yang et al., 2019) as a control. Vero cells were infected at an MOI of 1, followed 2h later by the addition of increasing concentrations of ivermectin. 22h later, cell supernatant was harvested and virus production quantified by plaque assays and RT-qPCR analysis.

The results show clearly that ivermectin is a potent inhibitor of WNV, with EC_{50} values of 0.8 μM (Fig. 4, left panels; see Table 2) for both infectious virus production (plaque assay) and viral replication (RT-qPCR). ZIKV (Asian/Cook Islands/2014) showed comparable results (Fig. 4, centre panels; see Table 2), with EC_{50} values of 1-2 μM, confirming that ivermectin is also able to inhibit this strain of ZIKV. These results for WNV and ZIKV were very similar to those for DENV2 (New Guinea C) (EC_{50} values of c. 0.5 μM; see Fig. 4, right panels); that ivermectin is not cytotoxic at the concentrations used here has been documented in a number of studies (Wagstaff et al., 2011, 2012; Tay et al., 2013). Finally, we confirmed IC50 analysis in the human disease-relevant peripheral blood mononuclear cell system (Supp. Fig. 5; Fraser et al., 2014), results (IC50 values of 1-3 μM) again underlining ivermectin's antiviral efficacy towards these viruses. Clearly, ivermectin is efficacious in limiting infection by a range of different flaviviruses, including WNV; since it is FDA approved and has an established safety profile in humans, ivermectin thus appears to be an interesting possibility to treat flaviviral disease, where there are currently no therapeutic alternatives.

3. Discussion

Insect-borne, flavivirus infections continue to rise worldwide, meaning that antivirals able to limit the growth of viruses such as DENV, ZIKV and WNV are urgently needed; ivermectin, first identified as a nuclear transport inhibitor by high throughput screening in 2011 (Wagstaff et al., 2011), is of considerable interest in this context in being able to limit infection by WNV, as shown here for the first time, as well as ZIKV and DENV (Fig. 4). Although ivermectin clearly has multiple effects on

eukaryotic cells as well as DENV proteins (Mastrangelo et al., 2012; Kosyna et al., 2015; Van der Watt et al., 2016), the present study clearly establishes for the first time that targets IMPα directly to alter its conformation and prevent interaction with IMPβ1, and thus block NLS recognition/nuclear targeting of DENV and ZIKV NS5, as well as host proteins (Kosyna et al., 2015). This adds to a growing body of literature documenting the viability of targeting viral protein nuclear import as a means to inhibit a range of viruses (Caly et al, 2012; Wagstaff et al., 2012, 2018; Tay et al., 2013; Lundberg et al., 2013; Fraser et al., 2014; Wang et al., 2017; Shechter et al., 2017; Atkinson et al., 2018; Lopez-Denman et al., 2018; Thomas et al., 2018; see Jans et al., 2019; Yang et al., 2019). In the case of flaviviruses in particular, three structurally distinct inhibitors – ivermectin, 4-HPR and GW5074 (see Yang et al., 2019) - have been described in some detail with respect to mechanism of action, all of which inhibit nuclear accumulation of NS5 in infected cells, and concomitantly limit flavivirus replication. As shown here using a range of different approaches, ivermectin targets the host factor IMPα, direct binding altering IMPα conformation to prevent interaction with IMPβ1 and hence NLS recognition, in a cellular context (Fig. 3), and thereby inhibit NS5 nuclear import, in analogous fashion to 4-HPR which prevents NS5 nuclear targeting through IMPα/β1 by binding selectively to NS5 itself (Fraser et al., 2014). Figure 5 summarises the different ways known inhibitors such as ivermectin and 4-HPR can block NS5-IMPα/β1 interaction to prevent NS5 nuclear translocation and its subsequent impact on the antiviral response/host mRNA splicing *etc.* (Medin et al., 2005; Pryor et al., 2007; Rawlinson et al., 2009; De Maio et al., 2016; Giovannoni et al. 2019; Ng et al., 2019). It should also be stressed that additional effects (not shown in Fig. 5) on host cell nuclear import (eg. Kosyna et al., 2015) and other processes (van der Watt et al., 2016) likely contribute to the antiviral action of ivermectin (and likely GW5074). Despite the potential for toxicity arising from effects on host processes (van der Watt et al., 2016), ivermectin has been shown to have an established safety profile for human use (see Jans et al., 2019), with existing pharmacokinetic data implying that concentrations of ivermectin suitable to limit flaviviruses could well be achievable without adverse-side effects using oral administration (eg. Guzzo et al., 2002; Gonzales Canga et al., 2008; Munoz et al., 2018). The fact that it is FDA-approved for parasitic infections (Gonzales Canga et al., 2008) makes it a particularly exciting possibility as a broad-spectrum antiviral for flaviviruses, as indicated by the fact that it is the focus of the Phase II/III trial currently recruiting in Thailand for DENV (NCT03432442). Further, it is also efficacious in inhibiting DENV replication in mosquitoes (see Xu et al., 2018).

The fact that ivermectin binding to the ARM repeat domain of IMPα not only inhibits IMPα recognition of nuclear targeting sequences through the ARM domain, but also binding to IMPβ1 mediated by the distinct N-terminal IBB domain of IMPα, is intriguing, these results being similar to those for the recently described inhibitor GW5074 (Yang et al, 2019), which although quite distinct in terms of structure, appears to have several properties in common with ivermectin. Ivermectin binding impacts IMPα thermostability and α-helicity, implying that it limits the inherent flexibility of the ARM repeat domain (Vihinen, 1987), thereby preventing binding to IMPβ1/NS5 *etc.*; protein flexibility (Alvarez-Garcia and Barril, 2014) is a key factor in enabling proteins such as IMPβ1 (Zachariae and Grubmuller, 2008) to bind to multiple binding partners, including diverse transport cargoes, as well as IMPα through its IBB domain, RanGTP and the hydrophobic repeats of the nucleoporins that make up the nuclear pore.

The ability of ivermectin to inhibit IMPα–NLS binding in a cellular context, is shown here for the first time using the BiFc system (Fig. 3). The results show that not only can the IMPα–NLS (and IMPαΔIBB–NLS) interaction be detected and quantified in a living cell, but also inhibited using a small molecule such as ivermectin. BiFc thus looms as a powerful system to analyse inhibitor effects in a cellular context, and conceivably has potential for development in the future as an assay to perform HTS for inhibitors of protein-protein interaction *in situ* in the living cell. This is an exciting possibility, meriting further investigation in the future.

In conclusion, the results here underline the viability of targeting viral protein nuclear transport to have an antiviral effect. In particular, our study highlights IMPα, and the IMPα/β1 binding interface, as robust candidate targets for the development of antivirals (see also Yang et al., 2019; Jans et al., 2019). Detailed crystallographic structures of inhibitors such as ivermectin with IMPα in the future will be an important priority to inform the therapeutic development of agents that can inhibit viral protein nuclear import, and yet have limited impact on host function, and circumvent issues of drug resistance. This remains a focus of future work in this laboratory.

4. Methods

4.1. Inhibitors

Ivermectin and budenoside were purchased from Sigma-Aldrich and *N*-(4-hydroxyphenyl) retinamide (4-HPR) from Tocris Bioscience.

4.2. Cell culture and virus propagation

Cells of the Vero African green monkey kidney and BHK-21 Baby hamster kidney lines were maintained in Dulbecco's modified eagle serum (DMEM) media supplemented with 10% heat-inactivated FBS at 37°C in a humidified incubator supplemented with 5% CO_2 (Wagstaff et al., 2012; Fraser et al., 2014). C6/36 *Aedes albopictus* cells were maintained in Basal Medium Eagle (BME) media supplemented with 10% heat-inactivated FBS at 28°C in a humidified incubator supplemented with 5% CO_2 (Fraser et al., 2014). Viral stocks of DENV-2 (New Guinea C; M29095) were propagated in C6/36 cells, and ZIKV (Asian/Cook Islands/2014) and WNV (MRM61C) in Vero cells as previously (Yang et al., 2019); cells at 80% confluency were infected at a multiplicity of infection (MOI) of 0.1. At 48 h, when > 70% of the cells were detached, the supernatant was harvested as the virus stock. Viral titre was subsequently determined by plaque assay (see below).

4.3 Protein expression

Recombinant proteins His_6-DENV2 (TSV101) NS5 (Wagstaff et al., 2012), His_6-DENV3 RdRp (Genbank accession AY662691), His_6-ZIKV RdRp (Brazil), and mouse His_6-IMPα2 with and without the IMPβ1-binding domain (residues 67–529; IMPαΔIBB) were expressed and purified by Ni^{2+}-affinity chromatography as previously (Yang et al., 2019). Mouse IMPα2 and mouse IMPβ1 proteins were expressed as GST fusion proteins and purified using glutathione S-beads as described (Fontes et al., 2003). Biotinylation of IMPs was carried out as previously (Wagstaff et al., 2011, 2012).

4.4 AlphaScreen

AlphaScreen binding assays were performed as previously (Wagstaff et al., 2011, 2012; see Yang et al., 2019). IC_{50} analysis was performed using 30 nM His_6-IMPα binding to 5 nM biotinylated-GST-IMPβ1; 30 nM His_6-DENV NS5 binding to 10 nM prebound His_6-IMPα/biotinylated-IMPβ1 heterodimer (Yang et al., 2019).

4.5 Analytical ultracentrifugation

Sedimentation velocity experiments were conducted using a Beckman Coulter Optima analytical ultracentrifuge at a temperature of 20°C as previously (Atkinson et al., 2018; Yang et al., 2019). The IMPα/β1 heterodimer was performed by incubating equimolar concentrations of the proteins at room temperature for 30 min in IMP binding (IB) buffer (110 mM KCl, 5 mM NaHCO3, 5 mM MgCl2, 1 mM EGTA, 0.1 mM CaCl2, 20 mM HEPES, 1 mM DTT, pH 7.4). Inhibitor or an equivalent volume of DMSO was added prior to centrifugation. 380 µl of sample and 400 µl of reference solution (PBS) were then loaded into a conventional double sector quartz cell and mounted in a

Beckman 8-hole An-50 Ti rotor. Samples were centrifuged at a rotor speed of 40,000 rpm and the data was collected continuously at multiple wavelengths (233, 280 and 450 nm). Solvent density (1.0052 g/ml at 20°C) and viscosity (1.0189 cP at 20°C), as well as estimates of the partial specific volume (0.7384 ml/g for IMPα/β1 at 20°C) were computed using the program SEDNTERP (Laue et al., 1992). Sedimentation velocity data were fitted to a continuous size [*c*(*s*)] distribution model using the program SEDFIT (Schuck, 2000; Atkinson et al., 2018).

4.6 Thermostability

The impact of inhibitor binding on thermostability using the fluorescent dye Sypro orange (Thermo Fisher) was as described (Yang et al., 2019) using a Rotor-Gene Q6 plex, programmed in *melt curve* mode. 2 or 5 µM recombinant protein in phosphate-buffered saline (PBS) was mixed with or without DMSO or compound, and then heated from 27° to 90°C at a rate of 1 °C/min (Yang et al., 2019). Fluorescence intensity due to Sypro orange binding was measured using excitation at 530 nm and emission at 555 nm, and the thermal melt point (T_m), representing the temperature at which 50% of the protein is unfolded (Gras et al., 2012), was plotted against inhibitor concentrations using GraphPad Prism 7 (Yang et al., 2019).

4.7 Circular dichroism spectroscopy

Circular dichroism (CD) spectra of IMPs (0.1 mg/ml) in PBS in the absence or presence of 10 uM ivermectin, budenoside or 4-HPR were analysed as previously (Yang et al., 2019) from 190 to 250 nm in a 1 mm quartz cuvette at 20°C using a Jasco J-815 CD spectrometer. The α-helical content was calculated from the ellipticity at 222 nm as described (Munoz et al., 1995; Yang et al., 2019). Mean ellipticity values per residue (θ) were calculated as $\theta = (3300 \times m \times \Delta A)/(lcn)$, where l is the path length (0.1 cm), n is the number of residues, m is the molecular mass in Daltons, and c is protein concentration in mg/ml.

4.8 Infectious assays

Quantitative reverse transcription polymerase chain reaction (qRT-PCR) to estimate the number of viral genomes was performed as previously (Yang et al., 2019). Analysis of infectious virus (plaque assay) was performed as described in Yang et al. (2019) using BHK-21 or Vero cells for DENV-2 for ZIKV/WNV respectively. For infections using peripheral blood mononuclear cells (PBMCs), cells were isolated from a healthy human donor by standard Ficoll-Paque (GE Healthcare) extraction, and then were infected with ZIKV or DENV at a MOI of 1 for 2 h, after which medium was replaced with fresh medium containing 2% FCS and the indicated concentration of ivermectin (Fraser et al.,

2014). Dose-response curves were plotted from the plaque number versus the log of the concentration of the test compounds. The lack of toxicity of ivermectin at the concentrations used has been extensively documented previously (Wagstaff et al., 2011, 2012; Tay et al., 2012; Yang et al., 2019).

4.9 Plasmid construction for bimolecular fluorescence complementation

Bimolecular fluorescence complementation (BiFc) based on protein-protein interaction bringing together the Venus N-terminal (VN-) and C-terminal (VC-) fragments to reconstitute Venus protein fluorescence (Kodama et al., 2010) was used for in cell assessment of direct interaction of IMPα2 with NS5 and a control molecule. In all cases, PCR-amplified sequences for the coding regions were inserted into EcoRI/KpnI restriction sites of plasmid vector pBiFC-VC155 (Addgene #22011) (Shyu et Al., 2006) and pBiFC-VN155(I152L) (Addgene #27097) (Kodama et al., 2010) via Gibson Assembly® Cloning Kit (New England Biolabs).

The coding sequences of IMPα2 and ΔIBBIMPα2 (lacking the importin-β-binding domain) were generated by PCR using the following primers (5'-GGCCAAGAATTCGGAACCAGGGTACTGTAAATTGG –'3 and 5'-CCGGTTGGTACCGAAGTTAAAGGTCCCAGGAGC–'3) inserted into EcoRI/KpnI restricted plasmid pBiFC-VC155. DENV2 (AY037116.1) NS5 was PCR amplified using primers 5´-CTTATGGCCATGGAGGCCCGAATTCAAGGAACTGGCAACACAGGAG –'3 and 5'-GCTCCCGCCACCTCCGGTACCCCACAAGACTCCTGCCTCTTCC –'3, and inserted into EcoRI/KpnI restricted plasmid pBiFC-VN155(I152L) via Gibson Assembly® Cloning Kit (New England Biolabs). For the 4xNLS construct, which contains four tandem copies of Simian virus SV40-derived sequence encoding amino acids 111-135 (SSDDEATADAQHAAPPKKKRKVEDP) was PCR amplified using primers 5'-CTTATGGCCATGGAGGCCCGAATTCCACACAGGAAACAGACCATG –'3 and 5'-GCTCCCGCCACCTCCGGTACCGTCACGACGTTGTAAAACGACGG –'3 and inserted into EcoRI/KpnI restricted pBiFC-VN155(I152L). The integrity of all constructs was confirmed by DNA sequence analysis.

4.10 Fluorescence imaging/image analysis for bimolecular fluorescence complementation

HeLa cells cultured on coverslips were transfected to express the indicated BiFc constructs (VN- and VC-), and stained with 0.8 μg/ml Hoechst 33342 (Invitrogen) prior to imaging by confocal laser scanning microscopy (Nikon C1 invert Confocal Microscope) using a 60× oil immersion objective. Quantitative analysis of the Venus fluorescence intensity reconstituted by molecular

complementation was performed using the ImageJ 1.52n public domain software. Nuclei were delineated from the Hoechst channel using the threshold command, and nuclear YFP fluorescence from Venus reconstitution, corrected for background in the absence of BiFc expression (non-transfected cell), then determined for 50-100 cells/sample.

4.11 Statistical analysis

Statistical analysis was performed using GraphPad Prism 7 software.

Acknowledgements

The authors acknowledge the financial support of the National Health and Medical Research Council Australia (Senior Principal Research Fellowship APP1002486/APP1103050; Project grant APP1043511; Development grant APP1117470; Early Career Fellowship APP1072267) and Australian Research Council (Future Fellowship #110100223). The Monash Micro Imaging Facility (Clayton) is acknowledged.

References

Alvarez-Garcia, D. and Barril, X., 2014. Molecular simulations with solvent competition quantify water displaceability and provide accurate interaction maps of protein binding sites. J. Med. Chem. 57, 8530-8539, http://dx.doi.org/10.1021/jm5010418.

Atkinson, S., et al., 2018. Recognition by host nuclear transport proteins drives disorder-to-order transition in Hendra virus V. Scientific Reports 8, 358. doi: 10.1038/s41598-017-18742-8.

Barrows, N.J., et al., 2016. A Screen of FDA-Approved Drugs for Inhibitors of Zika Virus Infection. Cell Host Microbe 20, 259-270.

Bhatt, S., et al., 2013. The global distribution and burden of dengue. Nature 496, 504-507.

Brady, O.J., et al., 2012. Refining the Global Spatial Limits of Dengue Virus Transmission by Evidence- Based Consensus. PLoS Negl Trop Dis 6, e1760. doi:10.1371/journal.pntd.0001760.

Caly, L., Wagstaff, K.M., Jans, D.A., 2012. Subcellular trafficking of pathogens: targeting for therapeutics. Antiviral Res. 95, 202-206.

Clinical Trials.gov [Internet]. Siriraj Hospital, Mahidol University, Bangkok, Thailand. Recruiting - Identifier NCT03432442, Pharmacokinetics and Pharmacodynamics of Ivermectin in Pediatric Dengue Patients. Available from: https://clinicaltrials.gov/ct2/show/NCT03432442?term=ivermectin&draw=2&rank=10.

De Maio, F.A., et al., 2016. The Dengue Virus NS5 Protein Intrudes in the Cellular Spliceosome and Modulates Splicing. PLoS Pathogens 12(8), e1005841.

Fontes, M.R., et al., 2003. Structural basis for the specificity of bipartite nuclear localization sequence binding by importin-alpha. J. Biol. Chem. 278, 27981-7.

Fraser, J.E., et al., 2014. A nuclear transport inhibitor that modulates the unfolded protein response and provides in vivo protection against lethal dengue virus infection. J. Infect. Dis. 210, 1780-91.

GBD 2015 HIV Collaborators, 2016. Estimates of global, regional, and national incidence, prevalence, and mortality of HIV, 1980–2015: the Global Burden of Disease Study 2015. Lancet HIV 3, e361–87.

Giovannoni, F., et al., 2019. Dengue nonstructural protein 5 polymerase complexes with promyelocytic leukemia protein (PML) isoforms III and IV to disrupt PML-nuclear bodies in infected cells. Front. Cell. Infect. Microbiol. 9, 284. doi: 10.3389/fcimb.2019.00284.

González Canga A., et al., 2008. The pharmacokinetics and interactions of ivermectin in humans - a mini-review. AAPS J. 10, 42–46.

Götz, V., et al., 2016. Influenza A viruses escape from MxA restriction at the expense of efficient nuclear vRNP import. Scientific Reports 6, 25428. doi: 10.1038/srep25428.

Gras, S., et al., 2012. A structural basis for varied alphabeta TCR usage against an immunodominant EBV antigen restricted to a HLA-B8 molecule. J. Immunol. 188, 311-321.

Guzzo, C.A., et al., 2002. Safety, tolerability, and pharmacokinetics of escalating high doses of ivermectin in healthy adult subjects. J. Clin. Pharmacol. 42, 1122-1133.

Hu, C.-D., Chinenov, Y., Kerppola, T.K., 2002. Visualization of Interactions among bZIP and Rel Family Proteins in Living Cells Using Bimolecular Fluorescence Complementation. Mol. Cell, 9**,** 789-798.

Hübner, S., Xiao, C-Y., Jans, D.A., 1997. The protein kinase CK2 site (Ser111/112) enhances recognition of the SV40 large T-antigen nuclear localization sequence by importin. J. Biol. Chem. 272, 17191-17195.

Jans, D.A., Martin, A., Wagstaff, K.M., 2019. Inhibitors of Nuclear Transport. Curr. Opin. Cell Biol. 58, 50-60.

Ji, W., Luo, G. 2020. Zika virus NS5 nuclear accumulation is protective of protein degradation and is required for viral RNA replication. Virology 541, 124-135.

Kerppola, T.K., 2008. Bimolecular fluorescence complementation (BiFC) analysis as a probe of protein interactions in living cells. Ann. Rev. Biophys. 37**,** 465-487.

Kobe, B., 1999. Autoinhibition by an internal nuclear localization signal revealed by the crystal

structure of mammalian importin alpha. Nat. Struct. Biol. 6, 388-397, http://dx.doi.org/10.1038/7625

Kodama Y., Hu C. D., 2010. An improved bimolecular fluorescence complementation assay with a high signal-to-noise ratio. BioTechniques 49, 793–805. 10.2144/000113519

Kosyna F.K., Nagel M., Kluxen L., Kraushaar K., Depping R., 2015. The importin α/β-specific inhibitor Ivermectin affects HIF-dependent hypoxia response pathways. Biol. Chem. 396, 1357–1367.

Laue, T.M., Shah, B.D., Ridgeway, T.M., Pelletier, S.L., 1992. Analytical Ultracentrifugation in Biochemistry and Polymer Science. The Royal Society of Chemistry, Cambridge, pp 90-125.

Lo, M.C., et al., 2004. Evaluation of fluorescence-based thermal shift assays for hit identification in drug discovery. Anal. Biochem. 332, 153-9.

Lopez-Denman, A.J., et al., 2018. Nucleocytoplasmic shuttling of the West Nile virus RNA-dependent RNA polymerase NS5 is critical to infection. Cell. Microbiol. 20, e12848. doi: 10.1111/cmi.12848.

Lundberg, L., et al., 2013. Nuclear import and export inhibitors alter capsid protein distribution in mammalian cells and reduce Venezuelan Equine Encephalitis Virus replication. Antiviral Res. 100, 662-72.

Major AT, et al., 2015. Specific interaction with the nuclear transporter importin α2 can modulate paraspeckle protein 1 delivery to nuclear paraspeckles. Mol. Biol. Cell. 26, 1543–58. doi: 10.1091/mbc.E14-01-0678.

Martin, A., Jans, D.A., 2018. Nucleocytoplasmic Trafficking of Dengue Non-structural Protein 5 as a Target for Antivirals. Adv. Exp. Med. Biol. 1062, 199-213.

Mastrangelo E. et al. 2012. Ivermectin is a potent inhibitor of flavivirus replication specifically targeting NS3 helicase activity: new prospects for an old drug. J. Antimicrob. Chemother. 67, 1884–1894.

Medin, C.L., K.A. Fitzgerald, Rothman, A.L., 2005. Dengue virus nonstructural protein NS5 induces interleukin-8 transcription and secretion. J. Virol. 79, 11053-61.

Munoz, V.; Blanco, F.J.; Serrano, L., 1995. The distribution of α-helix propensity along the polypeptide chain is not conserved in proteins from the same family. Protein Sci. 4, 1577–1586.

Munoz, J. et al., 2018. Safety and pharmacokinetic profile of fixed-dose ivermectin with an innovative 18mg tablet in healthy adult volunteers. PLoS Negl. Trop. Dis. 12, e0006020; doi: 10.1371/journal.pntd.0006020

Nair, H., et al., 2011. Global burden of respiratory infections due to seasonal influenza in young children: a systematic review and meta-analysis. Lancet 3, 1917-30. doi: 10.1016/S0140-6736(11)61051-9.

Ng, I.H.W., et al., 2019. Zika Virus NS5 Forms Supramolecular Nuclear Bodies That Sequester Importin-α and Modulate the Host Immune and Pro- Inflammatory Response in Neuronal Cells. ACS Infect. Dis. 5, 932-948. https://doi.org/10.1021/acsinfecdis.8b00373.

Ortblad, K.F., Lozano, R., Murray, C.J.L., 2013. The burden of HIV: insights from the Global Burden of Disease Study 2010. AIDS 27, 2003–2017.

Patel, L.R., Curran, T., Kerppola, T.K., 1994. Energy transfer analysis of Fos-Jun dimerization and DNA binding. Proc. Natl. Acad. Sci. USA 91**,** 7360-7364.

Pryor, M.J., et al., 2007. Nuclear localization of dengue virus nonstructural protein 5 through its importin alpha/beta-recognized nuclear localization sequences is integral to viral infection. Traffic 8, 795-807.

Rawlinson, S.M., et al., 2009. CRM1-mediated nuclear export of dengue virus RNA polymerase NS5 modulates interleukin-8 induction and virus production. J. Biol. Chem. 284, 15589-97.

Schuck, P., 2000. Size-distribution analysis of macromolecules by sedimentation velocity ultracentrifugation and lamm equation modeling. Biophys. J. 78, 1606-19.

Shechter, S., et al., 2017. Novel inhibitors targeting Venezuelan equine encephalitis virus capsid protein identified using In Silico Structure-Based-Drug-Design. Sci. Reports 7, 17705.

Shyu, Y.J., Liu, H., Deng, X., Hu, C.D., 2006. Identification of new fluorescent protein fragments for bimolecular fluorescence complementation analysis under physiological conditions. Biotechniques 40, 61–66.

Tan M.J.A. et al., 2019. The Potential Role of the ZIKV NS5 Nuclear Spherical-Shell Structures in Cell Type-Specific Host Immune Modulation during ZIKV Infection. Cells 8, 1519; doi:10.3390/cells8121519

Tay, M.Y., et al., 2013. Nuclear localization of dengue virus (DENV) 1-4 non-structural protein 5; protection against all 4 DENV serotypes by the inhibitor Ivermectin. Antiviral Res. 99, 301-6.

Thomas, D.R., et al., 2018. Identification of novel antivirals inhibiting recognition of Venezuelan equine encephalitis virus capsid protein by the Importin α/β1 heterodimer through high-throughput screening. Antiviral Res. 151, 8-19.

Van der Watt P.J., et al., 2016. Targeting the Nuclear Import Receptor Kpnβ1 as an Anticancer Therapeutic. Mol. Cancer Therapeutics 15, 560–573.

Vihinen, M., 1987. Relationship of protein flexibility to thermostability. Protein Eng. 1, 477-80.

Wagstaff, K.M., et al., 2018. Molecular dissection of an inhibitor targeting the HIV integrase dependent preintegration complex nuclear import. Cell. Microbiol. e12953.

Wagstaff, K.M., Rawlinson, S.M., Hearps, A.C., Jans, D.A., 2011. An ALPHAscreen based assay for high-throughput screening for specific inhibitors of nuclear import. J. Biomol. Screening 16, 192-200.

Wagstaff, K.M., Sivakumaran, H., Heaton, S.M., Harrich, D., Jans, D.A., 2012. Ivermectin is a specific inhibitor of importin α/β-mediated nuclear import able to inhibit replication of HIV-1 and dengue virus. Biochem. J. 443, 851–856.

Wang, C., et al., 2017. Nuclear import inhibitor N-(4-hydroxyphenyl) retinamide targets Zika virus (ZIKV) nonstructural protein 5 to inhibit ZIKV infection. Biochem Biophys Res Commun, 493, 1555-1559.

World Health Organisation, https://www.who.int/news-room/fact-sheets/detail/influenza-(seasonal) November 2018.

World Health Organisation, https://www.unaids.org/en/resources/fact-sheet 2018.

Xiao, C-Y., Hübner, S., Jans, D.A., 1997. SV40 large tumor-antigen nuclear import is regulated by the double-stranded DNA-dependent protein kinase site (serine 120) flanking the nuclear localization sequence. J. Biol. Chem. 272, 22191-22198.

Xu T-L. et al., 2018. Antivirus effectiveness of ivermectin on dengue virus type 2 in Aedes albopictus. PLoS Negl. Trop. Dis. 12, e0006934; https://doi.org/10.1371/journal.pntd.0006934.

Yang, S.N.Y., et al., 2019. Novel Flavivirus Antiviral That Targets The Host Nuclear Transport Importin α/β1 Heterodimer. Cells 8, 281; doi:10.3390/cells8030281.

Yasuda Y, Miyamoto Y, Yamashiro T, Asally M, Masui A, Wong C, Loveland KL, Yoneda Y. Nuclear retention of importin alpha coordinates cell fate through changes in gene expression. EMBO J. 2012; 31:83–94.

Zachariae, U., Grubmuller, H., 2008. Importin-beta: structural and dynamic determinants of a molecular spring. Structure 16, 906-915; http://dx.doi.org/10.1016/j.str.2008.03.007.

Figure Legends

Figure 1. Ivermectin inhibits binding of IMPα to IMPβ1 and can dissociate the IMPα/β1 heterodimer. A. AlphaScreen technology was used to determine the IC_{50} values for inhibition of IMPα binding to IMPβ1 as well as for dissociation of prebound IMPα/β1 heterodimer for ivermectin and budesonide. Data represent the mean +/- SD for triplicate wells from a single typical experiment, from a series of two independent experiments (see Table 1 for pooled data). **B.** Results from sedimentation velocity analytical ultracentrifugation experiments on purified recombinant IMPs in the absence or presence of ivermectin or budesonide. The continuous sedimentation coefficient distribution [$c(s)$] was plotted as a function of $s_{20,w}$ for IMPα, IMPβ1, and IMPα/β1 in the absence or presence of ivermectin (see also Supp. Fig. 2) or budesonide, as indicated. Residual plots are shown in insets. Data are from a single experiment, representative of a series of two independent experiments (see Supp. Table 1 for pooled data).

Figure 2. Ivermectin binding to the IMPα ARM repeat domain impacts thermostability and α-helicity. A. His_6-tagged IMP or DENV and ZIKV RdRp proteins were subjected to thermostability analysis in the absence or presence of increasing concentrations of ivermectin or 4-HPR (DMSO concentration kept constant throughout) to determine the Tm (^oC). **B.** The α-helical content of IMPα, IMPαΔIBB and IMPβ1 was analysed by CD spectroscopy in the presence of increasing concentrations of ivermectin. α-helical content was calculated from MRE data at 222 nm, as described in Methods (see Supp. Fig. 3 for CD spectra). Results shown (**A, B**) are from of a single experiment, representative of two independent experiments (see Supp. Table 2 for pooled data).

Figure 3. Ivermectin can inhibit interaction of IMPα with DENV NS5 in living cells. HeLa cells were transfected to express the indicated BiFc constructs, treated with either DMSO or ivermectin (25 μM) overnight, and imaged by CLSM 18 h post-transfection. **A.** Fluorescent images are shown,

with merge overlays of BiFc (yellow) and Hoechst nuclear stain (blue) on the right. **B.** Results for quantitation of specific nuclear fluorescence relative to VC-IMPα2 complementing with VN-4xNLS (left) VC-IMPα2 complementing with VN-NS5. Results represent the mean +/- SEM for a single typical experiment, from a series of 2 independent experiments. * $p < 0.05$; ** $p < 0.01$; *** $p < 0.001$; **** $p < 0.0001$.

Figure 4. Ivermectin is a potent anti-flaviral agent. Vero cells were infected with WNV, ZIKV or DENV at a MOI of 1 for 2 h, after which medium was removed, and fresh medium containing 2% FCS and the indicated concentration of ivermectin added. Culture medium was collected 22 h later and viral titres determined by plaque assay or qRT-PCR (Fraser et al., 2014; Yang et al., 2019). Results represent the mean +/- SD for duplicate wells from a single assay, representative of 2 (n=2) independent experiments. See Table 2 for pooled data.

Figure 5. Mode of action of different inhibitors blocking flavivirus NS5 nuclear import. In the absence of inhibitors (top), NS5 is recognised by the IMPα/β1 heterodimer, where IMPα interacts with IMPβ1 via the IBB domain of IMPα (green curved line), followed by nuclear import to impact host antiviral responses. Based on the results here, the IMPα targeting compound ivermectin appears to bind to IMPα (binding site shown as red lozenge) both within the IMPα/β heterodimer to dissociate it, and to free IMPα to prevent it binding to IMPβ1, thereby block NS5 nuclear import. The recently described molecule GW5074 (not shown) appears to have a close to identical mechanism (Yang et al., 2019) to that shown here for ivermectin. In contrast, the NS5 targeting compound 4-HPR binds to NS5 (binding site shown as violet circle) to prevent its recognition by the IMPα/β heterodimer, similarly blocking NS5 nuclear import. Antiviral action of the inhibitors is through preventing NS5 impacting mRNA splicing/the host antiviral response, thereby enabling the full host antiviral response; although not analysed in the present study (and not shown), Ji and Luo (2020)

recently reported that blocking nuclear accumulation of ZIKV NS5 using ivermectin or 4-HPR results in increased cytoplasmic degradation of NS5.

Table 1. Summary of binding and inhibitory data for ivermectin from AlphaScreen analysis.

Protein	Kd* (nM)	IC_{50}* (μM)
IMPα + β1[a]	5.4 +/- 1.1	7.1 +/- 1.6
IMPα/β1[b]	NA+	9.6 +/- 4.3
IMPα/β1 + DENV NS5[c]	0.8 +/- 0.2	1.2 +/- 0.5

*Results represent the mean +/- SD (n = 2) from analysis as per Fig. 1A/Supp. Fig. 1
+NA, not applicable
[a]IMPα+β, IMPα binding to IMPβ1
[b]IMPα/β, prebound IMPα/β1 heterodimer
[c] IMPα/β1+DENV NS5, prebound IMPα/β1 heterodimer binding to DENV2 NS5

Table 2. Summary of EC_{50} data for antiviral activity of ivermectin.

	EC_{50} (µM)*	
Virus	**WNV**	**ZIKV**
Plaque assay	0.5 +/- 0.3	1.6 +/- 0.7
RT-qPCR	1.1 +/- 0.4	1.3 +/- 1.3

*Results represent the mean +/- SD (n = 2) from analysis as per Figure 5.

Supplementary Data

Supplementary Figure Legends

Supp. Figure 1. Ivermectin inhibits DENV NS5 recognition by IMPα/β1. AlphaScreen technology was used to determine the IC_{50} for inhibition by ivermectin to inhibit binding of IMPα/β1 (10 nM) to His_6-DENV NS5 (30 nM). Data represent the mean +/- SD for triplicate wells from a single typical experiment (see Table 1 for pooled data).

Supp. Figure 2. Ivermectin does not alter the sedimentation properties of IMPα, IMPαΔIBB or IMPβ1. Sedimentation velocity AUC experiments were performed on purified recombinant IMPα, IMPαΔIBB and IMPβ1, in the absence or presence of the indicated concentrations of ivermectin. The continuous sedimentation coefficient distributions [$c(s)$] from subsequent data analysis were plotted as a function of $s_{20,w}$ for IMPs alone (black) or in the presence of 12.5 (grey) or 50 (green) μM ivermectin. The residual plots are shown in insets.

Supp. Figure 3. CD spectra for IMPs in the absence and presence of ivermectin or control molecules 4-HPR and budenoside. CD spectra were collected for IMPα, IMPαΔIBB and IMPβ1 in the absence (black) or presence of 30 μM ivermectin (green, left), 4-HPR (red, middle), or budenoside (blue, right) as indicated. The plots are representative of two independent experiments.

Supp. Figure 4. Fos-Jun interaction in living cells is dependent on the bZIP domain of Fos as shown using bimolecular fluorescence. HeLa cells transfected to express the indicated BiFc constructs, with or without treatment with DMSO or ivermectin (25 μM) (B) were CLSM imaged 18 h post-transfection. Images for YFP fluorescence (yellow, left panels) are shown together with merge overlays for the YFP images with Hoechst nuclear stain (blue, right panels). Results for quantitation of specific nuclear fluorescence relative to that for VC-cFos (wildtype) interaction with VN-cJun (right). Results represent the mean +/- SEM for a single typical experiment, from a series of two independent experiments. **** $p < 0.0001$.

Supp. Figure 5. Ivermectin is a potent anti-flaviral as shown in human PBMC infectious model. Peripheral blood mononuclear cells (PBMCs) were isolated from a healthy human donor by standard Ficoll-Paque (GE Healthcare) extraction. PBMCs cells were infected with ZIKV or DENV at a MOI of 1 for 2 h, after which medium was replaced with fresh medium containing 2%

FCS and the indicated concentration of ivermectin. Culture medium was collected 22 h later and viral titres determined by plaque assay (Fraser et al., 2014). Results represent the mean +/- SD (n = 2).

Supp. Table 1. Hydrodynamic properties of IMPs α, β1, and the IMPα/β1 complex in the absence and presence of inhibitors determined from AUC.

Protein/Inhibitor	M_r[a]	M[b]	$s_{20,w}$[c]	f/f_0[d]
IMPα2 no addition	58072	55344	3.5	2.4
+ 12.5 μM ivermectin		55985	3.4	2.3
+ 50 μM ivermectin		58438	3.7	2.5
IMPα2ΔIBB no addition	50884	48151	3.3	2.4
+ 12.5 μM ivermectin		47584	3.4	2.4
+ 50 μM ivermectin		46042	3.4	2.4
IMPβ1 no addition	98557	100192	5.3	2.1
+ 12.5 μM ivermectin		94980	5.3	2.1
+ 50 μM ivermectin		93510	5.2	2.1
IMPα2/β1[e] no addition	156629	155055	6.7	2.7
+ 12.5 μM ivermectin		154344	6.7	2.7
+ 50 μM ivermectin		156821	6.8	2.7
+ 12.5 μM budesonide		154310	6.5	2.7
+ 50 μM budesonide		154116	6.5	2.7

[a] Relative molecular weight calculated from the amino acid sequence.

[b] Molar mass determined from the ordinate maximum of $c(M)$ distribution best fits (data not shown).

[c] Standardized sedimentation coefficient taken from the ordinate maximum of the $c(s)$ distribution best fits (see Fig. 1; Supp. Fig. 2).

[d] Frictional coefficient calculated from $s_{20,w}$ using the $\overline{\nu}$ method employing SEDNTERP.

[e] Values for IMPα2/β1 are for the largest sedimenting species in the distribution.

Supp. Table 2. Percent α-helicity of IMPα, IMPβ and IMPαΔIBB calculated from CD analysis.

	DMSO	ivermectin (μM)		4-HPR (μM)		budenoside (μM)	
		10	50	10	50	10	50
IMPα	68.2 ± 1.1	59.2 ± 1.8	52.1 ± 1.7	67.8 ± 1.7	68.1 ± 2.1	68.1 ± 1.6	67.5 ± 1.9
IMPαΔIBB	66.4 ± 1.9	58.8 ± 1.7	53.4 ± 1.2	67.2 ± 1.5	66.2 ± 2.2	67.5 ± 1.7	66.3 ± 1.9
IMPβ1	70.5 ± 1.7	71.1 ± 0.2	71.5 ± 1.3	69.8 ± 1.8	70.7 ± 2.3	69.9 ± 1.5	70.0 ± 1.8

*Results are calculated from the ellipticity at 222 nm and represent the mean +/- SD (n = 2) from CD analysis (eg. Supp. Fig. 3).

Figure 1

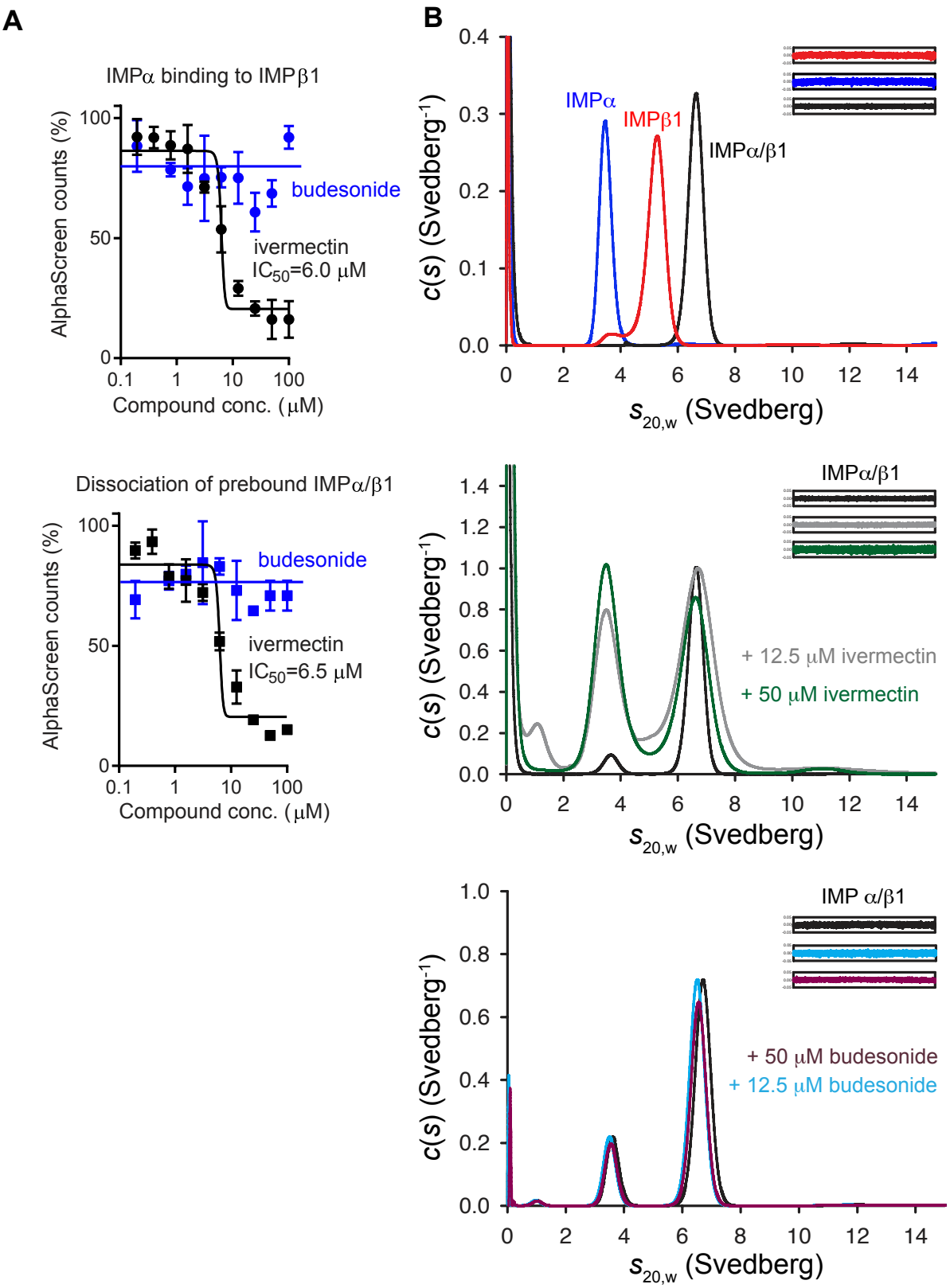
A
IMPα binding to IMPβ1
AlphaScreen counts (%)
100
50
0
0.1
1
10
100
Compound conc. (μM)
budesonide
ivermectin
IC50=6.0 μM
Dissociation of prebound IMPα/β1
AlphaScreen counts (%)
budesonide
ivermectin
IC50=6.5 μM
Compound conc. (μM)
B
c(s) (Svedberg-1)
IMPα
IMPβ1
IMPα/β1
s20,w (Svedberg)
IMPα/β1
+ 12.5 μM ivermectin
+ 50 μM ivermectin
IMP α/β1
+ 50 μM budesonide
+ 12.5 μM budesonide

Figure 2

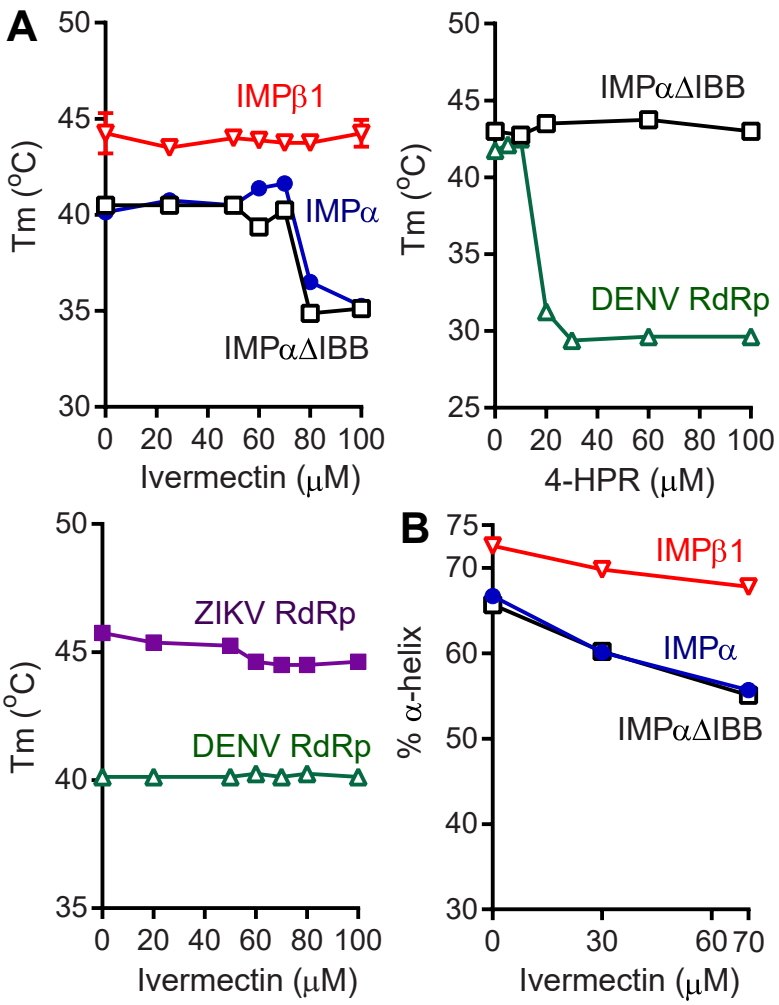
A
Tm (°C)
IMPβ1
IMPα
IMPαΔIBB
Ivermectin (μM)
IMPαΔIBB
DENV RdRp
4-HPR (μM)
ZIKV RdRp
DENV RdRp
Ivermectin (μM)
B
% α-helix
IMPβ1
IMPα
IMPαΔIBB
Ivermectin (μM)

Figure 3

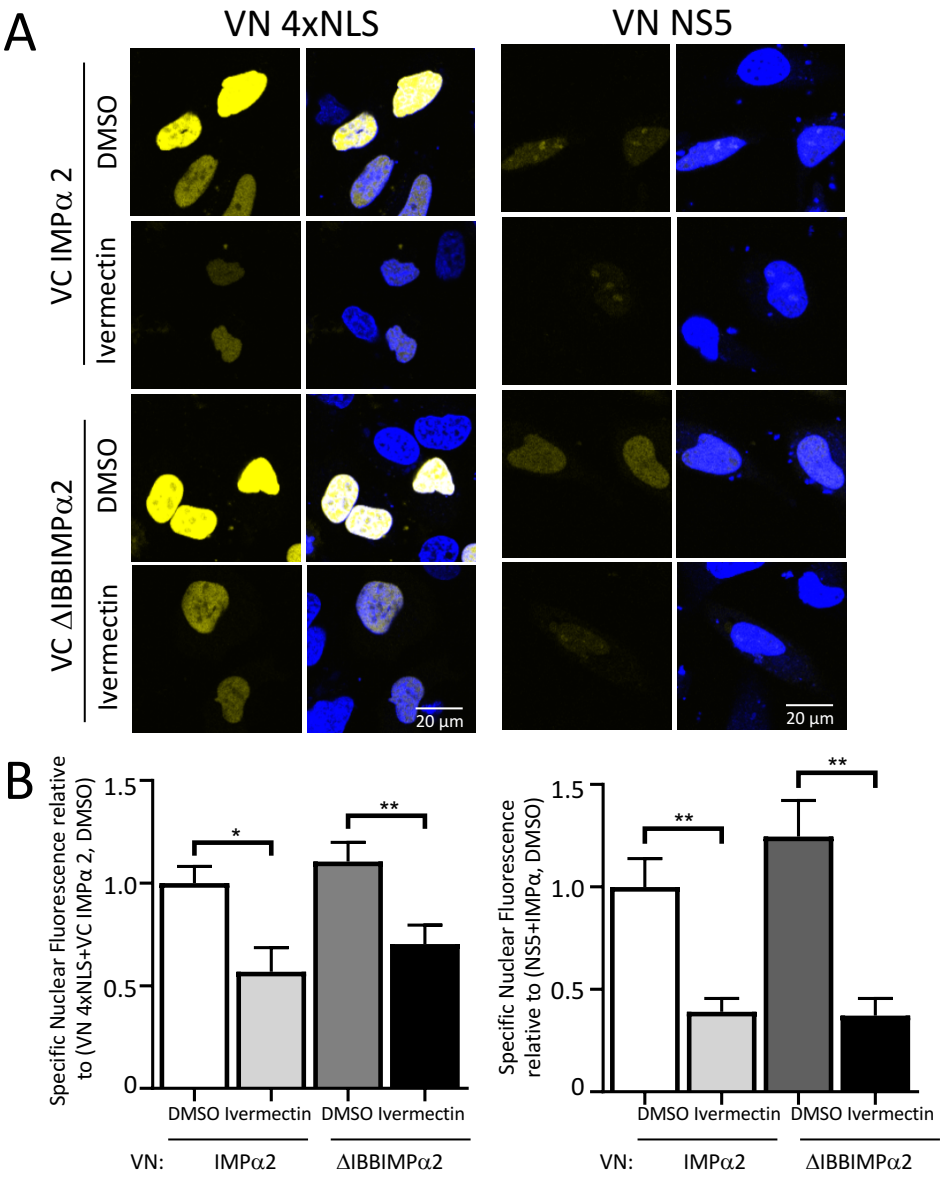
A
VN 4xNLS
VN NS5
VC IMPα 2
DMSO
Ivermectin
VC ΔIBBIMPα2
DMSO
Ivermectin
20 µm
20 µm
B
Specific Nuclear Fluorescence relative to (VN 4xNLS+VC IMPα 2, DMSO)
1.5
1.0
0.5
0
*
**
DMSO Ivermectin DMSO Ivermectin
VN: IMPα2 ΔIBBIMPα2
Specific Nuclear Fluorescence relative to (NS5+IMPα, DMSO)
1.5
1.0
0.5
0
**
**
DMSO Ivermectin DMSO Ivermectin
VN: IMPα2 ΔIBBIMPα2

Figure 4

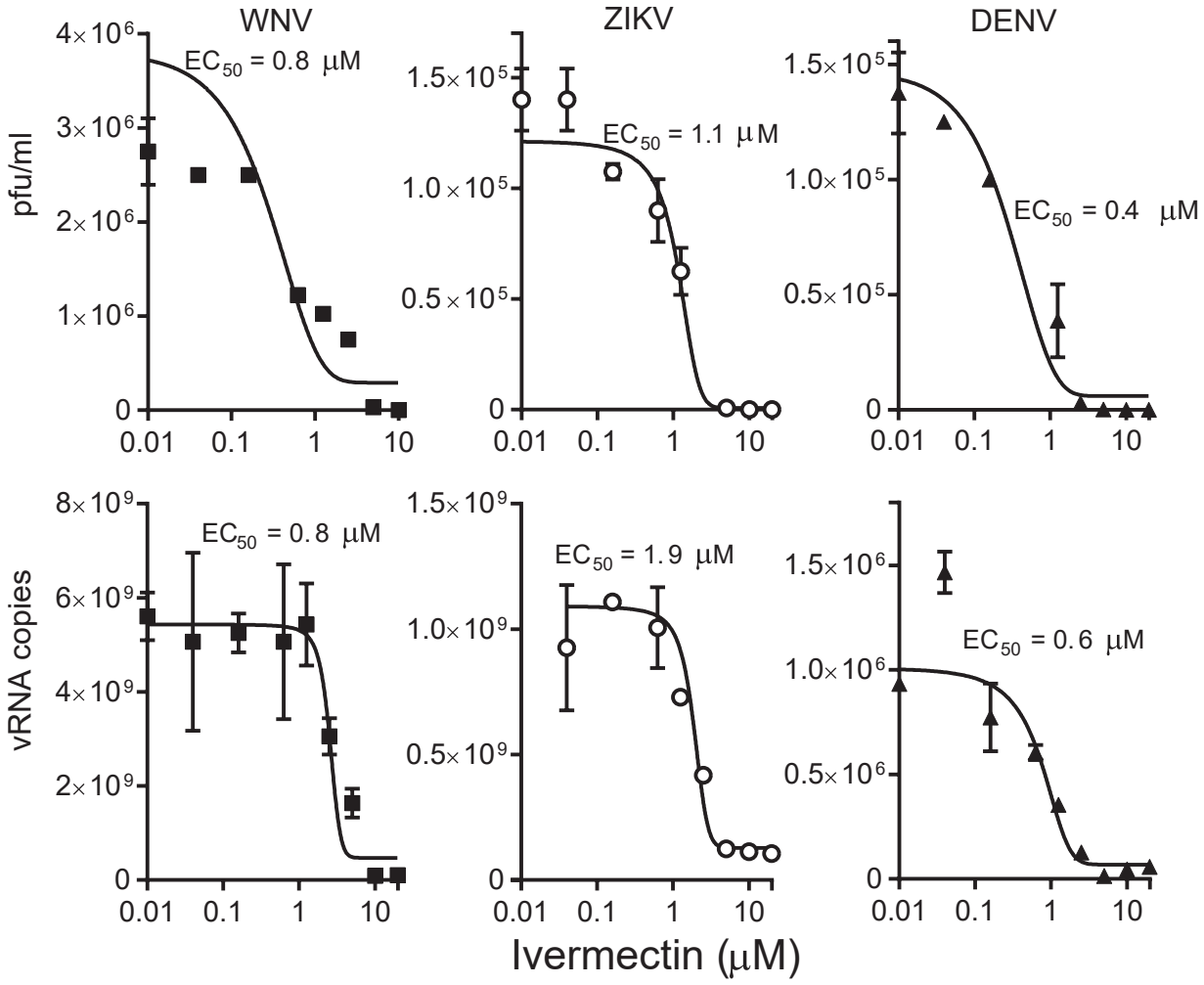
WNV
ZIKV
DENV
pfu/ml
vRNA copies
EC50 = 0.8 μM
EC50 = 1.1 μM
EC50 = 0.4 μM
EC50 = 0.8 μM
EC50 = 1.9 μM
EC50 = 0.6 μM
4×10^6
3×10^6
2×10^6
1×10^6
0
1.5×10^5
1.0×10^5
0.5×10^5
8×10^9
6×10^9
4×10^9
2×10^9
1.5×10^9
1.0×10^9
0.5×10^9
1.5×10^6
1.0×10^6
0.5×10^6
0.01
0.1
1
10
Ivermectin (μM)

Figure 5

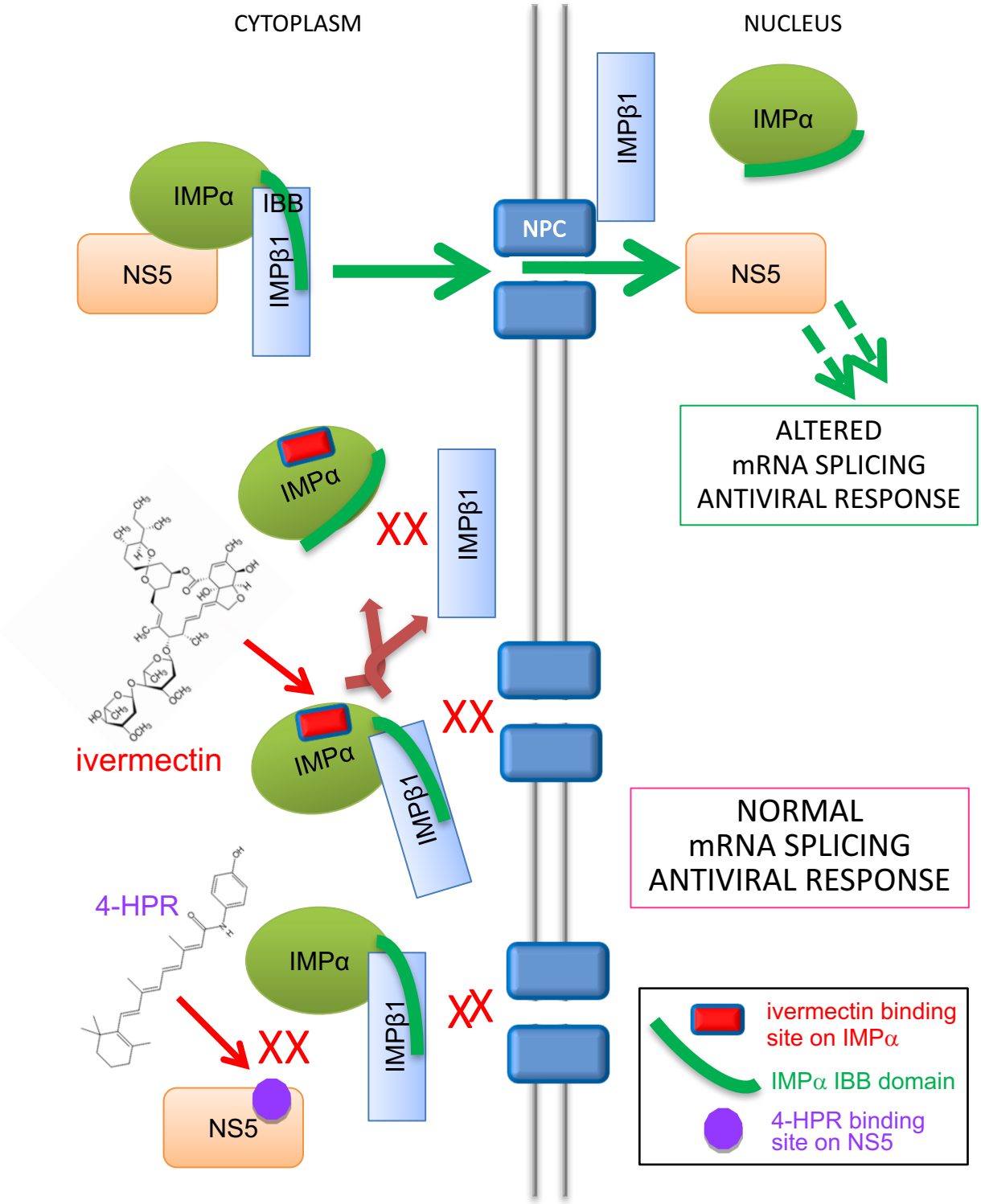
CYTOPLASM
NUCLEUS
IMPα
IBB
IMPβ1
NS5
NPC
IMPβ1
IMPα
NS5
ALTERED
mRNA SPLICING
ANTIVIRAL RESPONSE
IMPα
XX
IMPβ1
ivermectin
IMPα
XX
IMPβ1
NORMAL
mRNA SPLICING
ANTIVIRAL RESPONSE
4-HPR
IMPα
XX
IMPβ1
XX
NS5
ivermectin binding site on IMPα
IMPα IBB domain
4-HPR binding site on NS5

Supp. Figure 1

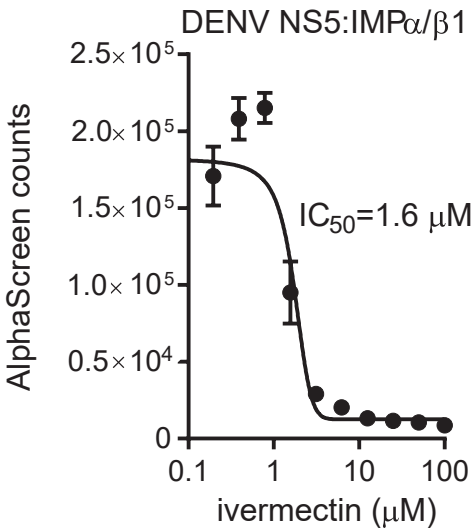

Supp. Figure 2

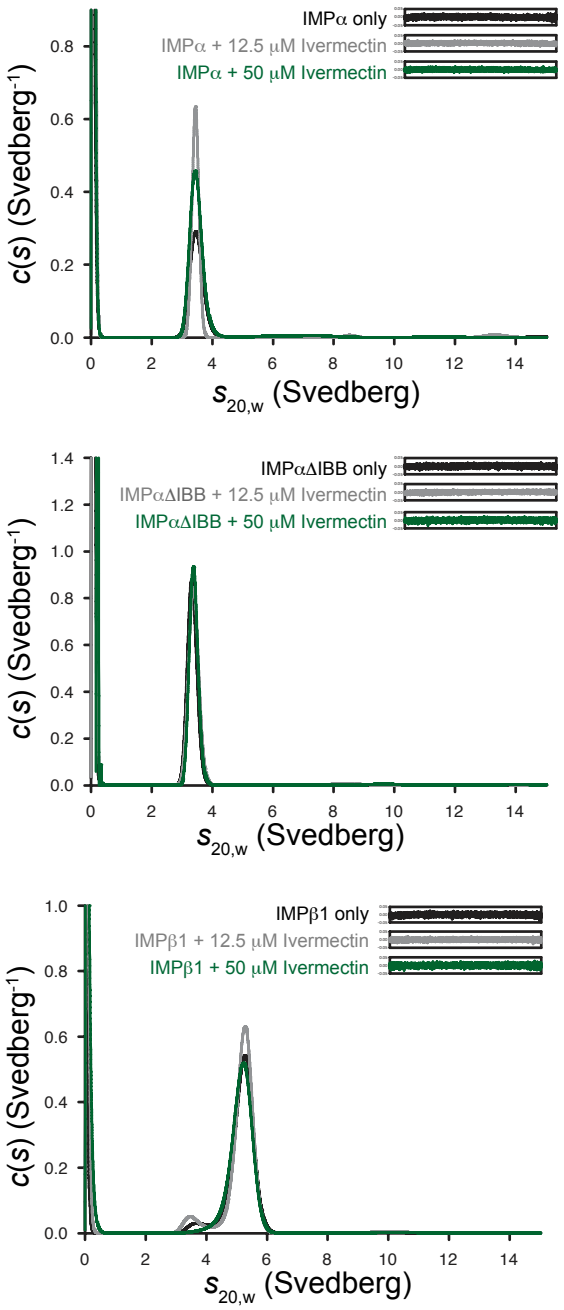

Supp. Figure 3

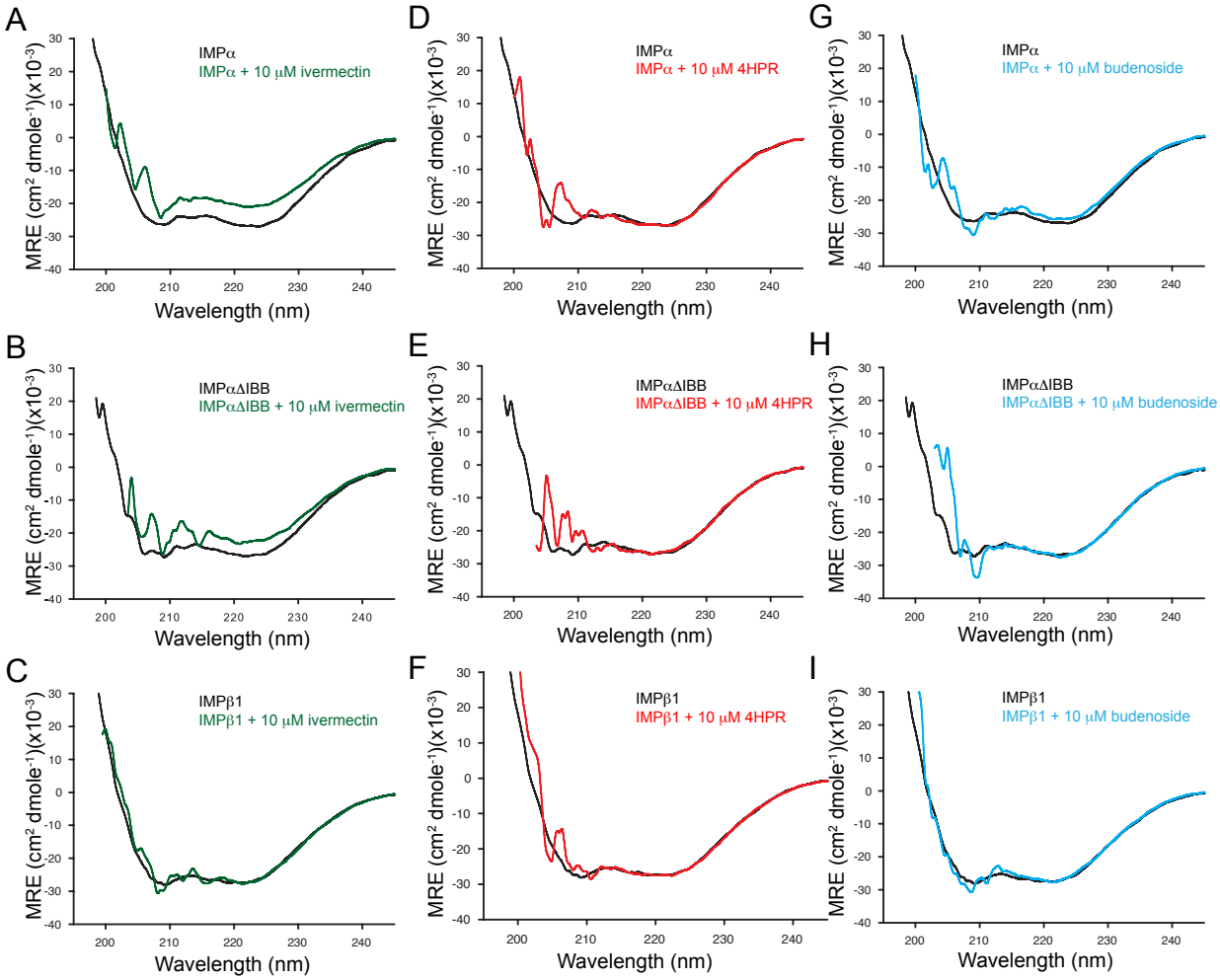

Supp. Figure 4

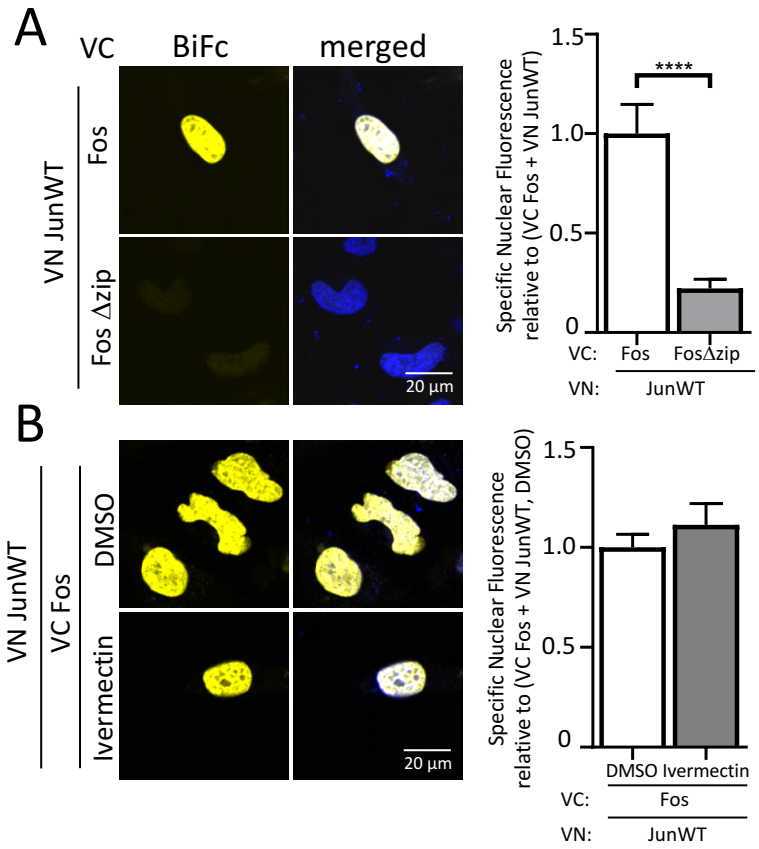

Supp. Figure 5

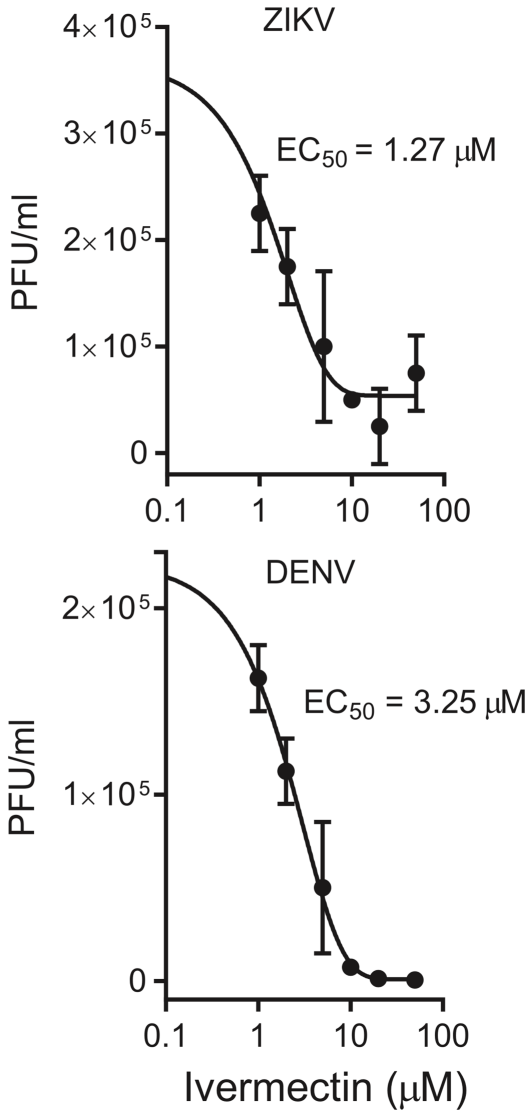

- The FDA-approved broad spectrum antiviral small molecule ivermectin targets host importin α/β1 heterodimer.
- Ivermectin can dissociate the host importin α/β1 heterodimer/prevent reassociation.
- Ivermectin can inhibity not only DENV, but also WNV and ZIKV, all of which are major burdens for human health.
- Ivermectin is a compelling prospect as a therapeutic for infection by flaviviruses and other pathogenic viruses.

Word count: 58